Effects of soil variability on settlement of a shallow foundation

Mohamad Nazieh Jlilati
Freelance researcher, Gifu, Japan

ABSTRACT
One of the distinguishing features of geotechnical reliability analysis, compared to other structural reliability analysis such as concrete and steel structures is material properties are different from site to site. The sources of uncertainties in reliability analysis are usually classified in four categories, namely physical uncertainty, model uncertainty, statistical uncertainty and gross error. The purpose of this study is to quantitatively evaluate the physical uncertainty, taking the settlement and the differential settlement prediction of a square shallow foundation on statistically homogeneous elastic ground, as an example.

RÉSUMÉ
L'un des dispositifs de distinction de l'analyse de fiabilité géotechnique, comparés à d'autres analyses de fiabilité structurale telle que les structures métalliques et en béton est que les propriétés matérielles sont différentes dun site a un autre. Les sources d'incertitudes dans l'analyse de fiabilité sont habituellement classées en quatre catégories, à savoir incertitude physique, incertitude modèle, incertitude statistique et erreur brut. Cependant, ce que nous observons dans la situation actuelle est un résultat combiné de toutes ces incertitudes. Le but de cette étude est d'évaluer quantitativement l'incertitude physique, prenant comme exemple une descente et la prévision d'une descente différentielle d'une fondation carrée peu profonde sur une terre élastique statistiquement homogène.

1 INTRODUCTION

In many of the textbooks in reliability design, the sources of uncertainties are classified in four categories, namely physical uncertainty, model uncertainty, statistical uncertainty and gross error (*e.g.* Thoft-Christensen and Barker, 1982). In the actual situation, it is observed that it is a combined result of all of these uncertainties. For example, when we check the accuracy of our prediction capability on the settlement of shallow foundations, what we observe are the differences between the observations and the predictions, and it is practically impossible to quantitatively identify each one of the four sources separately.

1.1 Objective and scope

The objective of this study is to quantitatively evaluate the physical uncertainty (*i.e.* spatial variability of soil properties) by taking settlement and the differential settlement prediction of a flexible square shallow foundation on elastic medium. The soil property (*i.e.* elastic modulus), is modeled as a random field. The lognormal distribution is assumed for soil variability with various autocorrelation distances. The Poisson ratio of the soil is set to be a deterministic value.

The resulting uncertainty due to spatial variability is evaluated by Monte Carlo simulation (MCS). Fenton and Griffiths (2002), Honjo et al. (2007), Jlilati and Honjo (2008) and others have studied the influence of the spatial variability on the settlement prediction. The methodology employed in this study is almost the same as one used by them, which is based on the random field theory (*e.g.* Vanmarcke, 1977, 1983) combined with the finite element method (Smith and Griffiths, 1987). However, the random field is generated in three-dimensions, so as to investigate 3-D effects on the settlement and differential settlement.

2 METHOD OF ANALYSIS

2.1 Procedure of study

A square footing on elastic ground whose Young's modulus, *E*, follow a homogeneous lognormal random field is considered. The settlement is evaluated by the finite element method, depending on the three-dimensional analysis using 8-node brick elements (Smith and Griffiths, 1987).

The procedure to evaluate settlement prediction uncertainty due to spatial variability is as follows:

1) A homogeneous standard normal random field is generated whose mean is zero, Standard deviation 1, and given autocorrelation distance (Shinozuka, 1971).

2) The generated Gaussian random field (RF) is transformed to the lognormal random field with given mean and standard deviation. In transforming the normal field to lognormal field, we alter the autocorrelation distance. However, it is not the exact value of the autocorrelation distance that the authors are interested to study but the generated influences. The same procedure is employed in Fenton and Griffiths (2002).

3) The transformed lognormal random field is assigned to the finite element mesh to evaluate the settlement of the square foundation on the specified load is evaluated.

4) The steps 1 through 3 are repeated until a sufficient number of results is obtained to evaluate the uncertainty.

The procedure above is repeated for different combinations of coefficient of variation of Young's modulus, COV_E, and the horizontal autocorrelation distances, a_h, while Poisson's ratio is assumed to be a constant (v=0.3).

2.2 Derivation of the solution

In this stage Young's modulus of the soil is assumed to consist of a heterogeneous but isotropic RF. Although soils generally exhibit a stronger correlation in the horizontal direction compared to the vertical, due to their layered nature, the degree of anisotropy is site specific (Fenton and Griffiths, 2002) and this point will be treated in later stages. The generation procedure of a RF is described as follow (Shinozuka, 1972). The autocorrelation function of the RF is assumed to be an exponential type:

$$C(r) = \exp[-\frac{r}{a}] \qquad [1]$$

where, *C(r)* is an autocorrelation function of an isotropic RF, and *r* is the distance between two points, and *a* is the autocorrelation distance.

Based on Wiener-Khintchine's citation, the autocorrelation function, *C(r)*, and the three-sided power spectrum function, *S(ω)*, has the following relationships (Christakos, 1992):

$$C(r) = 4\pi\int_0^\infty \frac{\sin(\omega r)}{r} S(\omega)\omega d\omega \qquad [2]$$

$$S(\omega) = \frac{1}{2\pi^2}\int_0^\infty \frac{\sin(\omega r)}{\omega} C(r) r dr \qquad [3]$$

where, *S(ω)* is a nonnegative bounded function, and *ω* is the frequency domain.
By applying "Eq. 3" to "Eq. 1"

$$S(\omega) = \frac{1}{2\pi^2}\int_0^\infty \frac{\sin(\omega r)}{\omega} \exp[-\frac{r}{a}] r dr \qquad [4]$$

On the other hand, based on Laplace - Euler transform:

$$\int_0^\infty e^{-cx} x^{\alpha-1}(\sin bx)dx = \frac{\Gamma(\alpha)}{(c^2+b^2)^{\alpha/2}}\sin(\alpha \arctan\frac{b}{c}) \qquad [5]$$

where α, b, and c are real numbers, and *Γ* is the Gamma function and it is defined as

$$\Gamma(\alpha) = (\alpha-1)! \qquad [6]$$

In case α = 2, "Eq. 5" takes the form:

$$\int_0^\infty e^{-cx} x(\sin bx)dx = \frac{\Gamma(2)}{c^2+b^2}\sin(2\arctan\frac{b}{c}) \qquad [7]$$

Where:

$$\Gamma(2) = (2-1)! = 1 \qquad [8]$$

so "Eq. 7" becomes:

$$\int_0^\infty e^{-cx} x(\sin bx)dx = \frac{1}{c^2+b^2}\sin(2\arctan\frac{b}{c}) \qquad [9]$$

by assuming c=1/*a*, b=*ω*, and applying "Eq. 9" to "Eq. 4"

$$S(\omega) = \frac{1}{2\pi^2\omega}\frac{1}{(\frac{1}{a})^2+\omega^2}\sin(2\arctan(a\omega)) \qquad [10]$$

Based on this power spectrum function and uniform random number *Φ*, a standard Gaussian random field *u(x, y, z)* can be generated as follows

$$u(x_{j_x}, y_{j_y}, z_{j_z}) = \sum_{k_x=1}^{N_x}\sum_{k_y=1}^{N_y}\sum_{k_z=1}^{N_z} a_{k_x k_y k_z}\cos(\omega_{xk_x} x_{j_x} + \omega_{yk_y} y_{j_y} + \omega_{zk_z} z_{j_z} + \Phi_{k_x k_y k_z}) \qquad [11]$$

Where:

$$a_{k_x k_y k_z} = \sqrt{2S(\omega)\Delta\omega_x\Delta\omega_y\Delta\omega_z} \qquad [12]$$

And *(x y, z)* is the coordinate of a point in space, *Φ* is a random phase angle uniformly and independently distributed in the interval (0,2*π*), and ω_x, ω_y and ω_z are the considered region in the frequency domain.

2.3 COMPUTING STEPS

Step 1: Generate 3-D Gaussian random field when mean=0 and variance=1, by Monte Carlo simulation.

Consider a 3-dimensional homogeneous random field with mean zero and spectral density function *S(ω)* which is of insignificant magnitude outside the region defined by

$$\omega_l \le \omega \le \omega_u \quad [13]$$

Denote the interval vector by

$$(\Delta\omega_x, \Delta\omega_y, \Delta\omega_z) = \left(\frac{\omega_{xl} - \omega_{xu}}{N_x}, \frac{\omega_{yl} - \omega_{yu}}{N_y}, \frac{\omega_{zl} - \omega_{zu}}{N_z}\right) \quad [14]$$

where N_x, N_y, N_z are the numbers of the intervals along the 3 axes of the wave number domain, and $\omega_l = -\omega_u$, therefore the interval vector could be written as

$$(\Delta\omega_x, \Delta\omega_y, \Delta\omega_z) = \left(\frac{2\omega_x}{N_x}, \frac{2\omega_y}{N_y}, \frac{2\omega_z}{N_z}\right) \quad [15]$$

Step 2: Transform the standard Gaussian field to a lognormal random field whose mean is μ_E and the standard deviation is σ_E .as a result, only the positive value of the Young's modulus, E, are generated. The mean and variance of lnE can be calculated as follows:

$$\sigma^2_{\ln E} = \ln\left(1 + \frac{\sigma^2_E}{\mu^2_E}\right) \quad [16]$$

$$\mu_{\ln E} = \ln \mu_E - \frac{1}{2}\sigma^2_{\ln E} \quad [17]$$

where μ_E is the mean of Young's modulus, and σ_E^2 is the variance of Young's modulus. The procedure proposed here is extended to anisotropic case. The sample is generated in the 3 directions, and Young's modulus is assumed to be the same for the horizontal and vertical directions. However the generated field is stretched in the horizontal direction only to give longer horizontal autocorrelation distance before assigning the generated random field to the finite element mesh to be calculated by FORTRAN program.

Step 3: The transformed lognormal random field is assigned to the finite element mesh to evaluate the settlement of the square foundation on the specified load.

Step 4: Repeat step 1 to 3 as many times as necessary.

The author considered 1000 times is sufficient in this research according to quick check for the results of simulating 100, 500, 1000, or 10000 times for one case.

3 NUMERICAL EXAMPLE

3.1 Description of cases analyzed

The soil mass is discretized into 19x19x19 eight-noded brick elements. While the overall dimensions of the ground model are *9.5D* by *9.5D* by *9.5D*, where *D* is the footing width. The size of the elements is *0.5D* by *0.5D* by *0.5D*. The side faces of the finite element model are constrained against horizontal displacement, but are free to slide vertically; while the nodes on the bottom boundary are fixed.

It seems there will be boundary effects associated with such close lateral boundary; therefore, the author has been evaluated the effect of the boundary condition by comparing the settlement obtained from his mesh and the settlement calculated by the Boussinesq equations. However, it is found that a vertical displacement in each element requested by the finite element method is almost corresponding to the Boussinesq's solution, and it could be confirmed that the finite element method program used by this research was appropriate.

To generalize the results, the calculation results are normalized by *q* (load intensity), and *D* as shown in Figure 1.

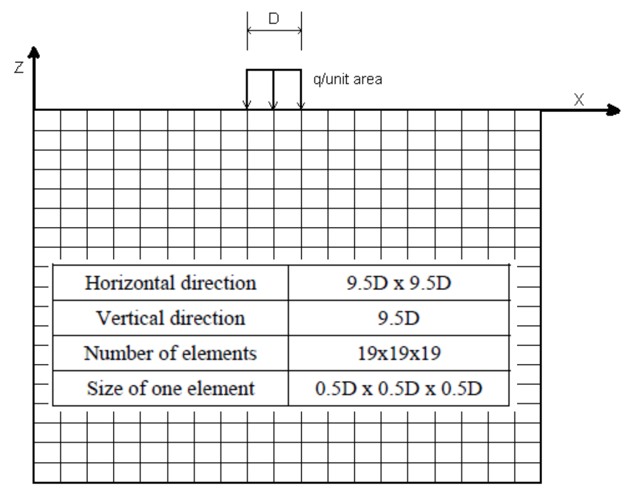

Figure 1. The ground setting and the loading conditions.

Young's modulus, *E*, is given by *E/q*, where E/q is 100. The settlement are normalized by *D*, where the ratio of the horizontal and vertical autocorrelation distant, a_h/a_v, is set to 1.0, 4.75, and 9.5. The COV_E is altered to 0.0, 0.3, 0.5, and 1.0. As a result, 12 different combinations of parameters are examined in total. 1000 Monte Carlo simulation runs are made for each case.

Table 1. Case studied for 3-D anisotropic evaluation of a shallow footing.

E/q	100
A_h/a_v [1]	1.0, 4.75, 9.5
COV_E	0.0, 0.3, 0.5, 1.0

[1] The vertical autocorrelation distance, a_v, is fixed to 1*D*.

It is actually necessary to consider the local averaging of the soil property depending on the mesh size as suggested by Vanmarcke (1977). At the same time, it is experienced that this problem is not terribly serious in practical calculation as shown by Suzuki (1990). The problem was not further studied in detail in this study.

4 RESULTS AND DISCUSSION

4.1 The settlement at the footing's center

Figure 2 shows the average settlement of the square footing, normalized by the width of the footing (μ_δ/D), against COV_E. It is observed that as the coefficient of variation of Young's modulus, COV_E, increases, the mean value of the settlement increases even though if the mean value of Young's modulus is the same.

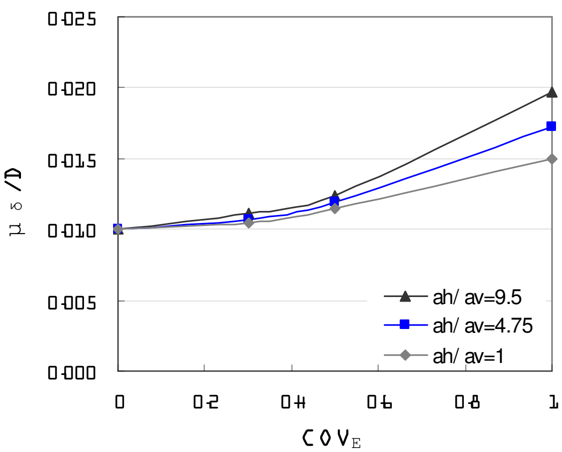

Figure 2. Relation of COV_E vs. Settlement (a_v=D).

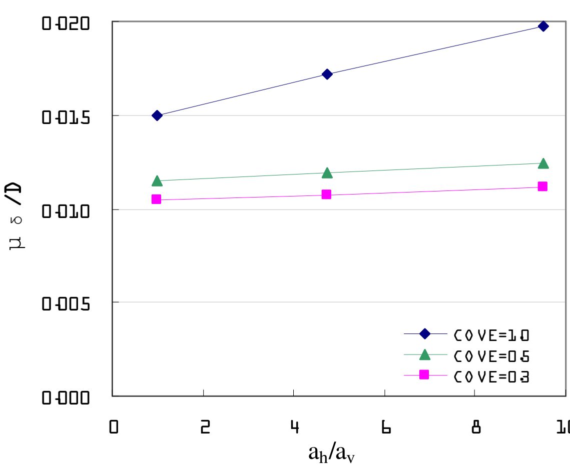

Figure 3. Relation of a_h/a_v vs. settlement (a_v=D).

Moreover, from Figure 3, the μ_δ/D increases as a_h/a_v increases and it appears to be a linear relation for fixed COV_E, a_v.

It is necessary here to call the results of some previous papers such as Fenton, and Griffiths (2002) and Honjo et al. (2007); it is found that the settlement, μ_δ/D, increases as COV_E increases, however, the settlement was independent of the autocorrelation distance. That was result of assuming the horizontal autocorrelation distance to be very long and varying the vertical autocorrelation distance. Therefore, this paper focused on varying the horizontal autocorrelation distance.

By combining the previous observation in this paper with Fenton, and Griffiths (2002) and Honjo et al. (2007) one can conclude that the relationship is independent of the vertical autocorrelation distance. However, this conclusion needs for further study.

In Figure 4 COV_δ/COV_E is plotted against a_h/a_v. It is observed that COV_δ/COV_E increases as a_h/a_v increases even if a_v is same. In other words, as the ratio of the autocorrelation distance increases the uncertainty of the predicted settlement (*i.e.* COV_δ/COV_E) increases. Moreover, it natural to observe some differences with changing COV_E, because the author studied the settlement, not the strain.

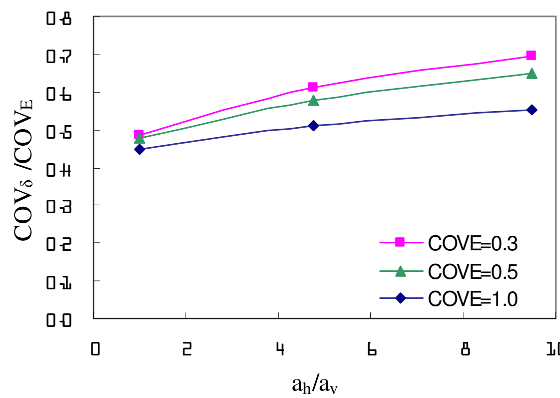

Figure 4. a_h/a_v vs. COV_δ/ COV_E (a_v=D).

4.2 The differential settlement

In many cases, the differential settlement is more serious than the absolute settlement itself; therefore, the second part of the results of the paper addresses the issue of the differential settlement. The differential settlement, Dif_δ, defined here as the maximum absolute inclination one can calculate considering the differential settlement values between the center of the footing and the corner nodes located at the edge of the footing divided by the distance between the two points.

$$Dif_\delta = Max\left[\ \left|\frac{(\delta_{center} - \delta_{corner\ i})}{D\sqrt{0.5}}\right|\ \right] \qquad [18]$$

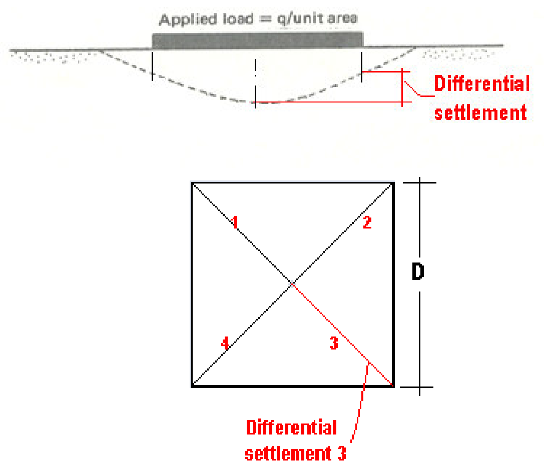

Figure 5. The differential settlement, Dif_δ.

It is important to recognize that the differential settlement can be caused by two factors:

1) Due to the uneven stress distribution at the center and the corner of the square footing.

2) Due to induced heterogeneity of Young's modulus of the ground, *E*.

As far as the first factor is concerned, the settlement at the center of the footing for the homogeneous ground, δ^*/D, is equal to 0.0101 (figure 2). In this condition the differential settlement, Dif_δ^*, is equal to 0.0077 (figure 6). Therefore, the ratio between the differential settlement and the settlement is 0.76 in this case (Dif_δ^*/δ^*= 0.0077/0.0101=0.76).

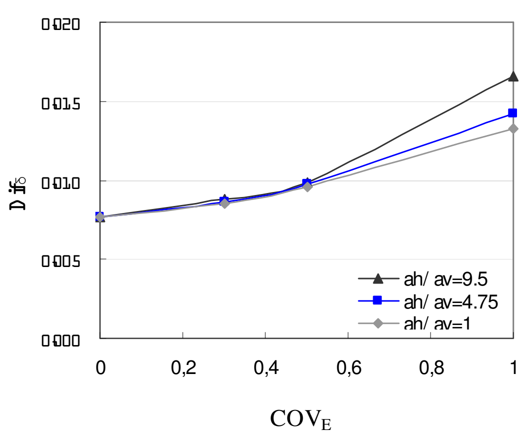

Figure 6. Relation of COV_E vs. differential settlement (a_v=*D*).

The ratio between Dif_δ and the settlement, however, ranged between 0.76 and 0.87 in this study for all cases; this is within the range where geotechnical engineers are using this ratio in practice. The reason for this small variation of this ratio in all cases is that the settlement also increases as the heterogeneity of the ground increases. Therefore, it is speculated that the empirical ratios are still valid in the heterogeneous ground, based on the results obtained in this study.

The effects of heterogeneity of the ground on the differential settlement are considerably large. The effect can be 10 to 100% of Dif_δ caused by the uneven stress distribution on the homogeneous ground (Dif_δ^* = 0.0077), depending on the ratio of the autocorrelation distance, a_h/a_v, and COV_E (for COV_E = 0.3 □1.0).

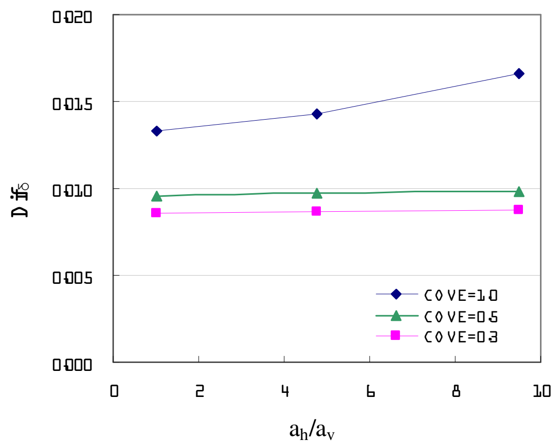

Figure 7. Relation of a_h/a_v vs. differential settlement (a_v=*D*).

From Figure 6 and Figure 7, it is observed that differential settlement increases as COV_E increases. It is also observed that a_h does not have much of an effect for small COV_E, and becomes more important for larg values of COV_E (heterogeneity).

From Figure 8, it is observed that $COV_{Dif\delta}/COV_E$ increases as a_h/a_v increases even if a_v is same. It is also natural to observe some differences with changing COV_E.

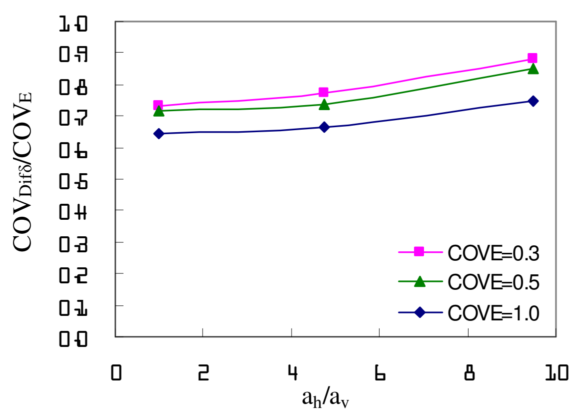

Figure 8. a_h/a_v vs. $COV_{Dif\delta}/COV_E$ (a_v=*D*).

5 CONCLUSIONS

The following conclusions can be drawn from this study:

It is observed that as the coefficient of variation of Young's modulus, COV_E, increases, the mean value of the settlement increases even though the mean value of Young's modulus is the same.

The differential settlement increases as COV_E increases, also it is observed that a_h has little effect for small COV_E, and becomes more important for large values of COV_E (heterogeneity).

As the ratio of the autocorrelation distance, a_h/a_v, increases the uncertainty of the predicted settlement (*i.e.* COV_δ/COV_E) and the uncertainty of the predicted differential settlement (*i.e.* $COV_{Dif\delta}/COV_E$) increases. Moreover, it natural to observe some differences with changing COV_E, because the author studied the settlement, not the strain.

The effects of heterogeneity of the ground on the differential settlement are significant. The effect can be 10 to 100% of Dif_δ caused by the uneven stress distribution on the homogeneous ground ($Dif_\delta^* = 0.0077$), depending on the ratio of the autocorrelation distance, a_h/a_v, and COV_E (for $COV_E = 0.3$ 1.0).

The ratio between Dif_δ and settlement ranged between 0.76 and 0.87 in this study for all cases; whereas 0.76 is obtained by the uneven stress distribution on homogeneous ground ($Dif_\delta^*/\delta^* = 0.0077/0.0101=0.76$). This is within the range where geotechnical engineers are using this ratio in practice. The reason for this small variation of this ratio in all cases is that the settlement also increases as the heterogeneity of the ground increases. Therefore, it is speculated that the empirical ratios are still valid in the heterogeneous ground, based on the results obtained in this study.

ACKNOWLEDGEMENTS

The writer would like to acknowledge the contribution of Professor Honjo Yusuke and Dr Mazari Azzedine to the paper.

REFERENCES

Fenton, G. A. and Griffiths, D. V. 2002. Probabilistic Foundation Settlement on Spatially Random Soil. *Journal of Geotechnic and Envairoment Engineering,* ASCE*,* 128(5):381-390.

George Christakos. 1992. *Random Field Models in Earth Sciences*: 69-71, 325-327.

Honjo, Y., Jlilati, M. N. & Ishino, J. 2007. Effects of Spatial Variability and Statistical Estimation Error in Prediction of Settlement of a Shallow Foundation. *ICASP10 '07,* Tokyo, Japan, 1: 173-174.

Jlilati, M. N. and Honjo, Y 2008. Effects of Spatial Variability of soil parameters on settlement of a Shallow Foundation. *Journal of Theoretical and Applied Mechanics*, (57): 49-56.

Shinozuka, M. 1972. Digital simulation of random processes and its applications. *Journal of sound and vibration* 25(1):111-128.

Shinozuka, M. 1971. Simulation of multivariate and multi dimensional random processes. *Journal of Acoustical Society of America*, 49(1) (Part2): 357-367.

Smith, I. M and Griffiths D. V. 1987. *Programming the Finite Element Method*. pp.182-186, John Wiley & Sons

Suzuki, M. 1990. *Probabilistic description of spatial distribution characteristics of geotechnical parameters and basic study on geotechnical reliability design*. Doctoral thesis submitted to Nagoya Institute of Technology.

Thoft-Chiridtensen, P. and M. J. Baker 1982. *Structural Reliability Theory and Its Application*, Springer-Verlag.

Vanmarcke, E. H. 1983. Random Field: analysis and synthesis, *The MIT press*.

Vanmarcke, E. H. 1977. Probabilistic modeling of soil profiles. *Journal of Geotechnical Engineering,* ASCE, 103(GT11):1227-1246.